

AD-A212 591

# NAVAL POSTGRADUATE SCHOOL

## Monterey, California



DTIC  
SELECTE  
SEP 21 1989  
S E D

# THESIS

MEASUREMENTS OF BUBBLE PROPERTIES  
USING A MULTI-FREQUENCY SOUND FIELD

by

Robert A. Perron

June 1989

Thesis Advisor: Anthony A. Atchley

Approved for public release; distribution is unlimited.

89 9 20 012

UNCLASSIFIED

SECURITY CLASSIFICATION OF THIS PAGE

## REPORT DOCUMENTATION PAGE

1a. REPORT SECURITY CLASSIFICATION UNCLASSIFIED			1b. RESTRICTIVE MARKINGS		
2a. SECURITY CLASSIFICATION AUTHORITY			3. DISTRIBUTION/AVAILABILITY OF REPORT		
2b. DECLASSIFICATION/DOWNGRADING SCHEDULE			Approved for public release, distribution is unlimited.		
4. PERFORMING ORGANIZATION REPORT NUMBER(S)			5. MONITORING ORGANIZATION REPORT NUMBER(S)		
6a. NAME OF PERFORMING ORGANIZATION Naval Postgraduate School		6b. OFFICE SYMBOL (If applicable) 61	7a. NAME OF MONITORING ORGANIZATION Naval Postgraduate School		
6c. ADDRESS (City, State, and ZIP Code)  Monterey, CA 93943-5000			7b. ADDRESS (City, State, and ZIP Code)  Monterey, CA 93943-5000		
8a. NAME OF FUNDING/SPONSORING ORGANIZATION		8b. OFFICE SYMBOL (If applicable)	9. PROCUREMENT INSTRUMENT IDENTIFICATION NUMBER		
8c. ADDRESS (City, State, and ZIP Code)			10. SOURCE OF FUNDING NUMBERS		
			PROGRAM ELEMENT NO.	PROJECT NO.	TASK NO.
			WORK UNIT ACCESSION NO.		
11. TITLE (Include Security Classification)  MEASUREMENTS OF BUBBLE PROPERTIES USING A MULTI-FREQUENCY SOUND FIELD <span style="float: right;">Unclassified</span>					
12. PERSONAL AUTHOR(S) Perron, Robert A.					
13a. TYPE OF REPORT Master's Thesis		13b. TIME COVERED FROM _____ TO _____		14. DATE OF REPORT (Year, Month, Day) June 1989	
15. PAGE COUNT 63					
16. SUPPLEMENTARY NOTATION					
17. COSATI CODES			18. SUBJECT TERMS (Continue on reverse if necessary and identify by block number)		
FIELD	GROUP	SUB-GROUP	Bubble Resonance Frequency, Nonlinear Bubble Dynamics, Rise-Time Bubble Sizing, Dual Frequency, Rectified Diffusion Damping, <i>etc.</i>		
19. ABSTRACT (Continue on reverse if necessary and identify by block number) An apparatus was designed, constructed, and tested to measure properties of single bubbles in a fluid by use of a multi-frequency sound field. The theoretical background on the dual frequency method for obtaining bubble properties such as resonance frequency, rectified diffusion thresholds and rates, rise-time sizing, and damping coefficients are discussed. Specifications and design of the device are presented. Sizes of single air bubbles in water determined from dual frequency methods are compared to rise-time sizing for radii from 30 to 100 $\mu\text{m}$ , these two methods are shown to agree within 1%. Rectified diffusion rates measured above, at, and below threshold for an initial bubble radius of 50 $\mu\text{m}$ in air-saturated water over a period of 700 seconds were measured and the results demonstrate the reliability of the system. The potential of this device to measure damping coefficient is discussed.					
20. DISTRIBUTION/AVAILABILITY OF ABSTRACT <input checked="" type="checkbox"/> UNCLASSIFIED/UNLIMITED <input type="checkbox"/> SAME AS RPT <input type="checkbox"/> DTIC USERS			21. ABSTRACT SECURITY CLASSIFICATION UNCLASSIFIED		
22a. NAME OF RESPONSIBLE INDIVIDUAL Anthony A. Atchley, Code 61Ay			22b. TELEPHONE (Include Area Code) (408) 646-2848		22c. OFFICE SYMBOL 61Ay

Approved for public release; distribution is unlimited.

Measurement of Bubble Properties Using a  
Multi-Frequency Sound Field

by

Robert A. Perron  
Captain, Canadian Forces  
B.S., Royal Roads Military College Canada, 1981

Submitted in partial fulfillment of the  
requirements for the degree of

MASTER OF SCIENCE IN ENGINEERING ACOUSTICS

and

MASTER OF SCIENCE IN PHYSICS

from the

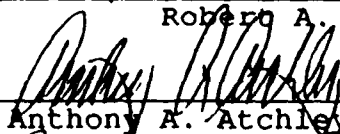
NAVAL POSTGRADUATE SCHOOL  
June 1989

Author:



Robert A. Perron

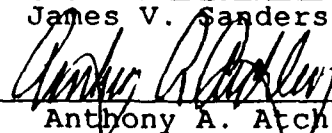
Approved by:




Anthony A. Atchley, Thesis Advisor



James V. Sanders, Second Reader



Anthony A. Atchley, Chairman  
Engineering Acoustics Academic Committee



Karlheinz E. Woehler, Chairman  
Department of Physics



Gordon E. Schacher  
Dean of Science and Engineering

## ABSTRACT

An apparatus was designed, constructed, and tested to measure properties of single bubbles in a fluid by use of a multi-frequency sound field. The theoretical background on the dual frequency method for obtaining bubble properties such as resonance frequency, rectified diffusion thresholds and rates, rise-time sizing, and damping coefficients are discussed. Specifications and design of the device are presented. Sizes of single air bubbles in water determined from dual frequency methods are compared to rise-time sizing for radii from 30 to 115  $\mu\text{m}$ , these two methods are shown to agree within 1%. Rectified diffusion rates measured above, at, and below threshold for an initial bubble radius of 50  $\mu\text{m}$  in air-saturated water over a period of 700 seconds were measured and the results demonstrate the reliability of the system. The potential of this device to measure damping coefficient is discussed.

Accession For  
NTIS GRA&I  
DTIC TAB  
Unannounced  
Justification  
By  
Distribution /  
Availability Codes  
Avail and/or  
Dist Statement



## TABLE OF CONTENTS

I.	INTRODUCTION . . . . .	1
II.	THEORY . . . . .	4
	A. DUAL FREQUENCY METHOD . . . . .	4
	B. RESONANCE FREQUENCY . . . . .	9
	C. SIZING OF BUBBLES BY RISE TIME . . . . .	11
	D. RECTIFIED DIFFUSION . . . . .	12
	E. FREQUENCY RESPONSE, DAMPING AND QUALITY FACTOR . . . . .	18
III.	APPARATUS AND MEASUREMENTS . . . . .	21
	A. DESIGN CONSIDERATIONS . . . . .	21
	1. Generating Bubbles . . . . .	23
	2. Bubble Levitation . . . . .	23
	3. Carrier and Exciter . . . . .	24
	4. Reception and Display of Received Signal . . . . .	24
	B. EXPERIMENTAL SETUP . . . . .	24
	1. Transducers . . . . .	25
	2. Apparatus . . . . .	27
	3. Electronic Equipment . . . . .	28
	4. Sample Fluid . . . . .	30
	5. Calibration . . . . .	30
	6. Procedures . . . . .	31

IV.	RESULTS AND DISCUSSION . . . . .	33
A.	SPECTRUM ANALYZER . . . . .	33
B.	BUBBLE RADIUS . . . . .	35
C.	RECTIFIED DIFFUSION . . . . .	38
D.	DAMPING COEFFICIENTS . . . . .	40
V.	SUMMARY . . . . .	49
	LIST OF REFERENCES . . . . .	50
	INITIAL DISTRIBUTION LIST . . . . .	51

## LIST OF TABLES

Table 1.	Threshold Acoustic Pressures Amplitudes for Rectified Diffusion of Various Air Bubbles in Air Saturated Water Driven at Resonance	. 15
----------	---	------

## LIST OF FIGURES

Figure 1.	Theoretical Sum Frequency Pressure, $P_1$ , and Exciter Frequency Echo Pressure, $P_2$ , for Air Bubble in Water with $f_0 = 20$ kHz, Curve a: $P_1$ and Curve b: $P_2$ . . . . .	8
Figure 2.	Equilibrium Radius for Air Bubble in Water . . . . .	10
Figure 3.	Sizing of Air Bubble in Water using Rise Time Method . . . . .	13
Figure 4.	Rectified Diffusion Measurements by Crum . . . . .	17
Figure 5.	Transducer Locations for Multi-Frequency Method . . . . .	26
Figure 6.	Multi-Frequency Method Setup . . . . .	29
Figure 7.	Frequency Spectrum with Bubble Carrier and Levitation Transducers On . . . . .	34
Figure 8.	Frequency Spectrum with Bubble Carrier, Exciter and Levitation Transducers On . . . . .	36
Figure 9.	Bubble Radius as Determined from Two Different Methods . . . . .	37
Figure 10.	Behavior of Air Bubble in Water when Applied Sound Field Less than Rectified Diffusion Threshold, $f = 21.9$ kHz, $P = 7.6$ kPa . . . . .	39
Figure 11.	Superposition of Five Frequency Spectrums, 100 Seconds Apart, at Rectified Diffusion Threshold . . . . .	41
Figure 12.	Bubble Radius Variations at Rectified Diffusion Threshold for Air Bubble in Water, $f = 21.9$ kHz, $P = 23.0$ kPa . . . . .	42



Figure 13. Superposition of Five Frequency Spectrums, 100 Seconds Apart, for Positive Rectified Diffusion . . . . .	43
Figure 14. Behavior of Air Bubble in Water when Applied Sound Field Greater than Rectified Diffusion Threshold, $f = 21.9$ kHz, $P = 30.4$ kPa . . .	44
Figure 15. Comparison of Exciters, Small Ceramic Transducers (heavy line), Panametrics V301 (thin line) . . . . .	46
Figure 16. Bubble Response from Small Ceramic Exciter .	47
Figure 17. Bubble Response from Small Ceramic Exciter .	48

## ACKNOWLEDGEMENT

I would like to express my gratitude to the following people for their help during my thesis research.

I would like to first thank my Thesis Advisor, Anthony A. Atchley, for his encouragement, dedication and insight of which I was a direct and avid recipient.

I would also like to express my heartfelt thanks to my fellow classmates in UX 73 for their support and friendship during my entire tour at NPS.

And, last but not least, to my wife Claudine who gave life to our son Remi during the production of this work; your sacrifices and encouragements are deeply appreciated.

## I. INTRODUCTION

The propagation of sound in water is significantly affected by the presence of bubbles. In order to be able to predict the propagation of sound in bubbly media, the dynamics of bubbles must be fully understood. The reason that bubbles have such a strong influence on propagation is their ability to absorb and scatter sound. The importance of these attenuation mechanisms is determined by the resonance frequency and damping coefficient of the bubbles, quantities which are related to the bubble's radius and frequency response.

A number of articles have appeared in the literature over the past decade or so pertaining to these aspects of the dynamics of gas bubbles in water. The majority of these studies are numerical computations of such things as: the frequency response of bubbles subjected to large amplitude sound fields, the variation of the instantaneous radius of the bubble with time, and the variation of the position of a bubble in the levitating sound field as a function of its radius. Although there have been some experimental

confirmations of these predictions, it is fair to say that experiment is well behind theory.

The most fruitful experimental techniques involve acoustically levitating a bubble, thereby allowing extended periods of observation. Two methods of observation have been proven particularly successful. The first involves visually observing the bubble through a telescope and measuring, as functions of the amplitude and frequency of the drive signal, either the position of the bubble in the sound field or its average radius via its rise velocity [Ref. 1]. This technique is tedious and places a great emphasis on the skill of the observer. In addition, the kinds of information are limited. The second technique employs illuminating a bubble with a laser and measuring the intensity of the scattered light [Ref. 2]. This technique takes the burden off the observer at the expense of a more complex experimental setup. In addition, the data must be inverted by the use of Mie scattering theory to infer the bubble radius. Nonetheless, this technique has great potential. In particular, it can yield the instantaneous radius of a bubble, a very desirable quantity.

A different observation technique is addressed in this thesis. It is based on a bubble-sizing method, developed by Newhouse and Shankar [Ref. 3], using the nonlinear mixing of

two frequencies (dual frequency method) which can yield the same information that is available through visual observations, but with much less effort on the part of the observer. It can also provide information about the frequency response of the bubble, which is not attainable through visual observations. In the present configuration of this observation technique, it is not possible to obtain the instantaneous radius of the bubble.

The theory necessary to understand the detection technique, as well as the measurements performed, are presented in the next chapter. Next the design of the measuring device and the associated experimental setup are discussed. The results of measurements of bubble radius, growth rate, and frequency response are then presented and discussed. The thesis concludes with a summary.

## II. THEORY

The goal of this thesis is to develop the frequency method of investigating the dynamics of bubbles. In particular, it is desired to determine the size of a bubble, its growth rate when exposed to a sound field, and its damping coefficient. The first two quantities can be determined from measurements of the resonance frequency of the bubble. The last quantity can be determined by measuring the radiated acoustic pressure amplitude as a function of driving frequency.

The principle behind the dual frequency method is given in the next section, followed by a discussion of the resonance frequency of a bubble. Then a description is given of an alternate method of determining the size of a bubble by measuring the time required for it to rise through a known distance. Next, the theory governing the growth rates of bubbles in sound fields, "rectified diffusion", is presented. The chapter concludes with a discussion of the frequency response and damping coefficient of bubbles.

### A. DUAL FREQUENCY METHOD

The majority of research, both experimental and theoretical, pertaining to bubble dynamics has considered the

problem of a bubble excited by a monofrequency sound field. The fundamental equation describing this phenomena is the Rayleigh-Plesset equation [Ref. 4: eq. 4, p. 122] which is a nonlinear equation expressing the radius of the bubble as a function of time.

$$\rho R \ddot{R} + \frac{3}{2} \rho \dot{R}^2 = (P_o + \frac{2\sigma}{R_o}) (\frac{R_o}{R})^{3\eta} - (P_o + \frac{2\sigma}{R}) - 4\mu \frac{\dot{R}}{R} + P_1 \cos \omega_1 t \quad (\text{eqn. 1})$$

where

$\rho$  = density of the liquid

$\mu$  = viscosity of the liquid

$\sigma$  = surface tension

$R_o$  = equilibrium bubble radius

$R$  = instantaneous bubble radius

$P_o$  = ambient pressure amplitude

$P_1$  = incident sound pressure amplitude

$\eta$  = polytropic exponent [ $1 < \eta < \gamma$  (ratio of specific heats)]

$\omega_1$  = angular frequency of the sound field

The dots indicate time derivative. The derivation of the Rayleigh-Plesset equation assumes that the bubble can be treated as a highly compressible, spherical body immersed in an incompressible fluid. All terms are expressed as energy per unit volume. The kinetic terms are displayed on the left end side of the equation. The first term of the right end

side represents contributions from thermal processes. The following two terms are the effects of surface tension and viscous stress of the bubble surface. The last term represents the energy resulting from the driving force.

The method used in this thesis involves two sound fields. This dual frequency method is described by including a second driving term  $P_2 \cos \omega_2 t$  on the right-hand side of the Rayleigh-Plesset equation. Newhouse and Shankar [Ref. 3] gives an extensive treatment of bubble response under the influence of two sound fields of different frequencies,  $f_1$  and  $f_2$ .  $f_1$  is much higher than the bubble's resonance frequency, but with a wavelength in the fluid still much longer than the diameter of the bubble.  $f_2$  is at or near the bubble's resonance frequency. The bubble is excited into large amplitude resonant oscillations by  $f_2$  while also responding to  $f_1$ , although with a much smaller oscillation amplitude.

Because the behavior of a bubble undergoing large amplitude oscillations is nonlinear, the bubble radiates sound not only at the incident frequencies  $f_1$  and  $f_2$ , but also at the sum  $(f_1+f_2)$  and difference  $(f_1-f_2)$  frequencies. All other possible combinations are also radiated, but with much lower amplitudes.



When the frequency  $f_2$  equals the resonance frequency of the bubble  $f_0$ , the radiated pressure amplitude  $(f_1+f_2)$  is given by Newhouse and Shankar [Ref. 3: eqn. 21, p. 1475].

$$P_+ = \frac{P_1 P_2}{\rho \omega_0^2 R_0 \delta r} \quad (\text{eqn. 2})$$

where

$P_1$  = acoustic pressure amplitude at the frequency  $f_1$  at the location of the bubble

$P_2$  = acoustic pressure amplitude at the frequency  $f_2$  at the location of the bubble

$P_+$  = acoustic pressure amplitude at the frequency  $(f_1+f_2)$  at the location of the receiver

$\omega_0$  = angular resonance frequency of bubble

$\delta$  = damping coefficient

$r$  = range from bubble to receiver

One advantage of the dual frequency method over monofrequency methods is that the sum and difference frequencies are generated only by resonant bubbles as shown in Figure 1. Hence, it is not sensitive to larger nonresonant bubbles or solid contaminants in the water. The reason is that the generation of the sum frequency requires that the bubble be undergoing large amplitude, nonlinear oscillations. Even though the backscattered pressure from the bubble peaks, dips, and rises linearly as shown in curve b of Figure 1, the sum and different frequencies  $(f_1+f_0)$  or  $(f_1-f_0)$ , are strong for only one bubble size as shown in curve a.

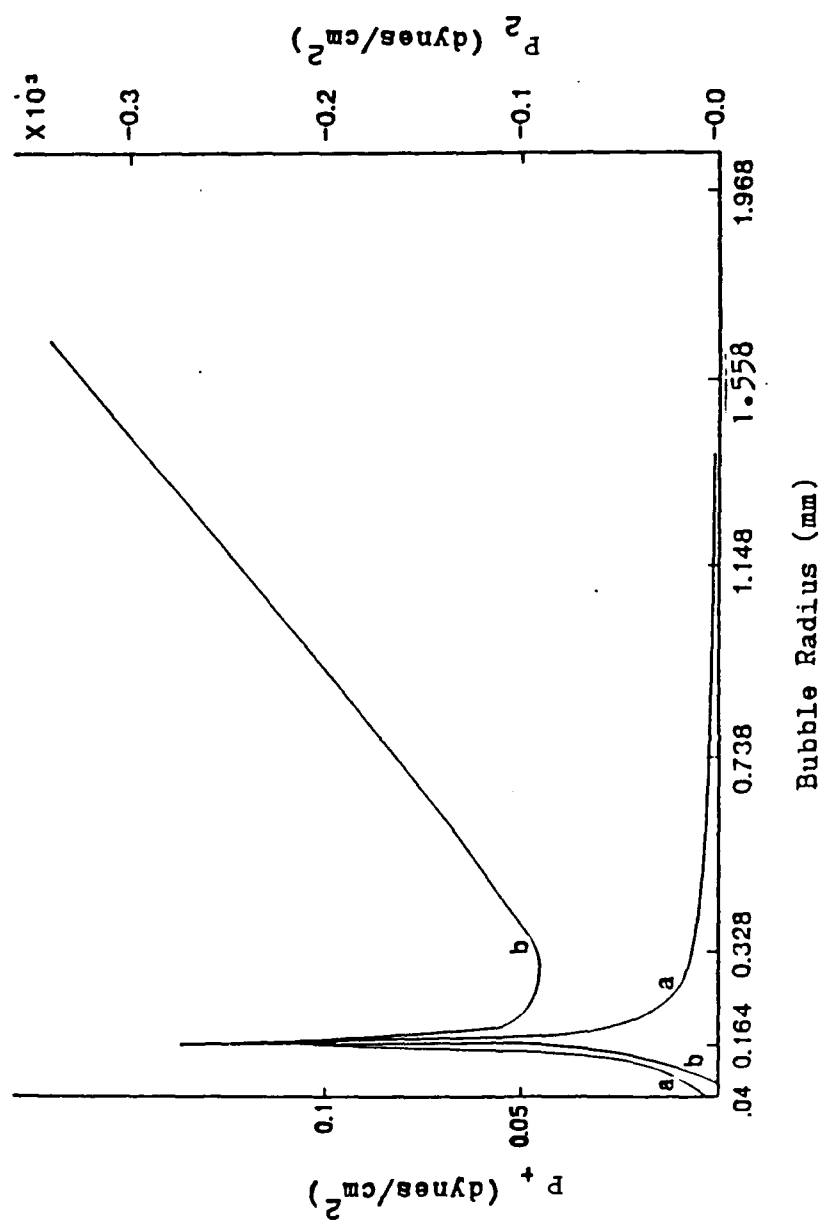


Figure 1. Theoretical Sum Frequency Pressure,  $P_+$ , and Exciter Frequency Echo Pressure,  $P_2$ , for Air Bubble in Water with  $f_0 = 20$  kHz, Curve a:  $P_+$  and Curve b:  $P_2$ .

## B. RESONANCE FREQUENCY

The concepts of bubble resonance and resonance frequency are crucial to the dual frequency method. Therefore it is worthwhile reviewing them. Devin gives the linear second order differential equation of motion for a bubble [Ref. 5: eq. 19, p. 1656].

$$\left(\frac{\rho}{4\pi R_o}\right)\ddot{v} + b\dot{v} + \left(\gamma \frac{P_o}{V_o}\right)v = -P \exp(j\omega t) \quad (\text{eqn. 3})$$

where

$v$  = change in volume from the equilibrium bubble volume

$b$  = dissipation coefficient

$\gamma$  = ratio of specific heats

$V_o$  = equilibrium bubble volume

$P$  = forcing pressure amplitude

If the dissipation is negligible, equation 3 gives the resonance frequency of the bubble [Ref. 5: eq. 21, p. 1656]

$$f_o = \frac{1}{4\pi R_o} \left( \frac{3\gamma P_o}{\rho} \right)^{1/2} \quad (\text{eqn. 4})$$

which is often called Minnaert's expression. Figure 2 is a graphical representation of equation 4 for air bubbles in

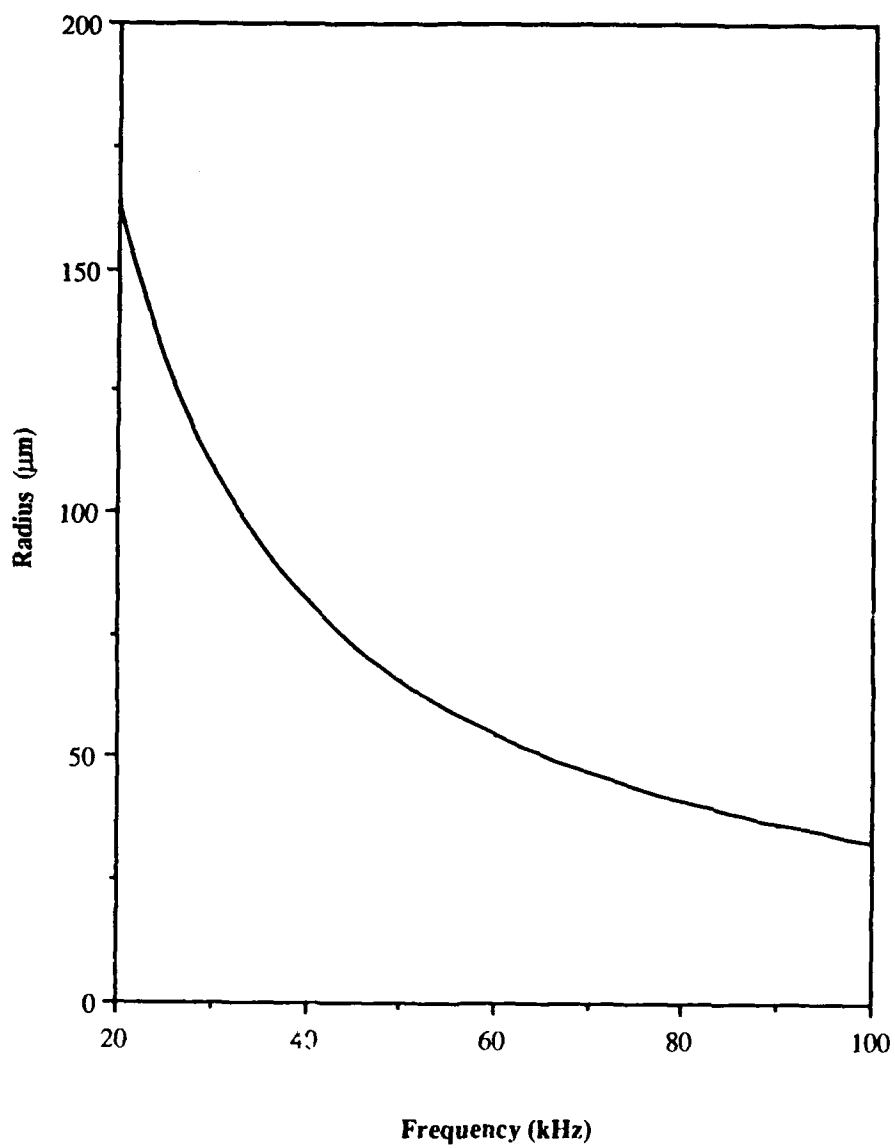


**Figure 2. Equilibrium Radius for Air Bubble in Water**

water. Surface tension has been neglected in this discussion because its effects are unimportant for bubble sizes of interest in this study.

### C. SIZING OF BUBBLES BY RISE TIME

In order to verify the dual frequency technique, an alternate method of determining bubble size is necessary. A relatively accurate method of finding the radius of a bubble is to measure the time required for a bubble to rise through a known distance in still water under the influence of buoyancy.

As documented in [Ref. 6], a bubble rises at constant speed due to the balance between buoyancy and drag forces. Since these forces depend on radius differently, the speed of a bubble varies with radius.

The terminal rise speed of a bubble is [Ref. 6]

$$U = \left[ \frac{8ag}{3C_D} \right]^{1/2} \quad (\text{eqn. 5})$$

where

U = rise speed

a = bubble radius

g = acceleration due to gravity

C<sub>D</sub> = drag coefficient

The drag coefficient developed by Schiller and Nauman was used for these computations [Ref. 6:eq. 4, p. 6]

$$C_D = \frac{24}{R_e} (1 + 0.15 R_e^{0.687}) \quad (\text{eqn. 6})$$

where

$R_e$  = Reynold's number =  $2aU/v_f$

$v_f$  = kinematic shear viscosity of fluid

Figure 3 displays the bubble radius relative to the time for a bubble to rise 25 mm in water. This method is not valid for bubble radii smaller than 15  $\mu\text{m}$  since the size is too small to be observed.

#### D. RECTIFIED DIFFUSION

In order to determine the utility of the dual frequency techniques, one measurement we can make is of the growth rates of bubble exposed to a sound field. The sound field will cause the bubble to grow (or dissolve) by a process known as rectified diffusion. Crum [Ref. 7] gives a detailed discussion of the subject. Rectified diffusion involves the slow growth of a pulsating gas bubble due to an average mass flow into the bubble as a function of time. The growth of a bubble can be detected by the associated change in its resonance frequency. The threshold acoustic pressure for growth of a gas bubble is [Ref. 7:eq. 19, p. 217]

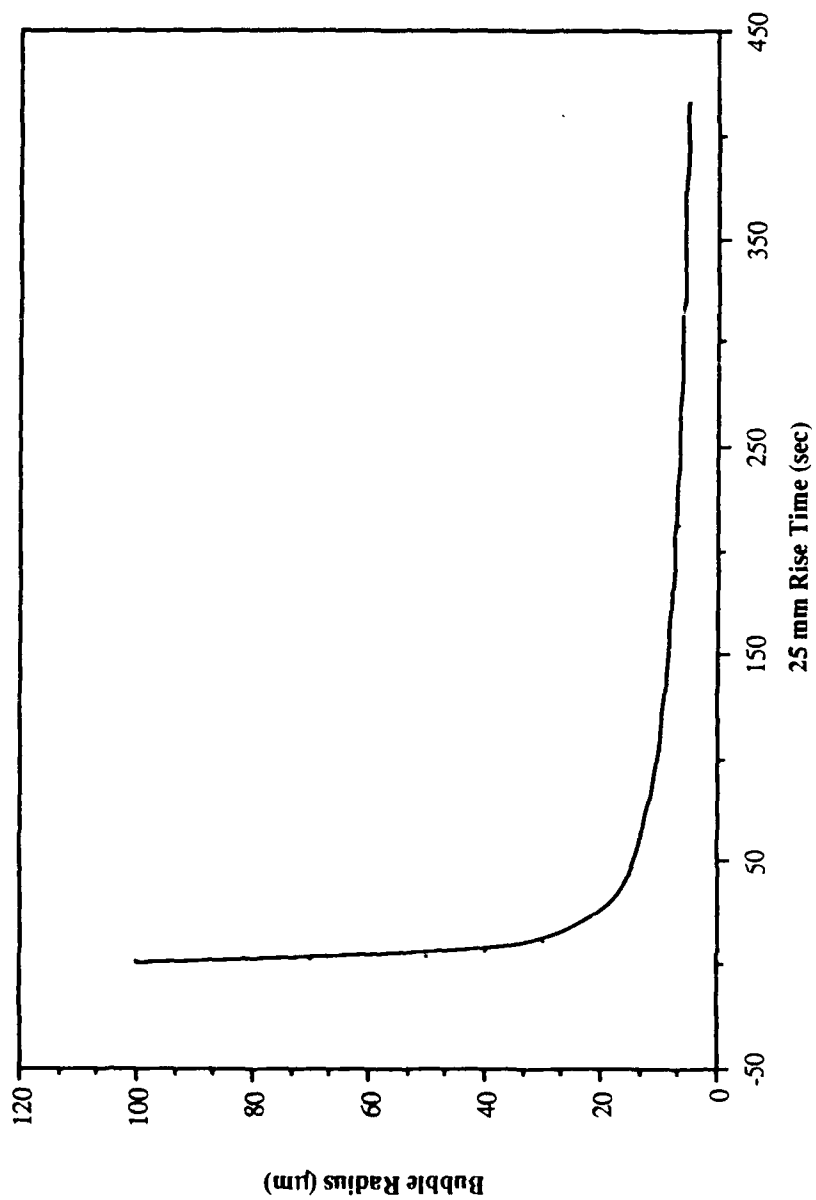


**Figure 3. Sizing of Air Bubble in Water Using Rise Time Method**

$$P_{th} = \frac{(\rho R_o^2 \omega^2) [(1 - (\frac{\omega}{\omega_o})^2)^2 + \delta^2 (\frac{\omega}{\omega_o})^2] (1 + \frac{2\sigma}{R_o P_o} - \frac{C_i}{C_o})}{(3 + 4K)(\frac{C_i}{C_o}) - \{ [\frac{3(\eta - 1)(\eta - 4)}{4}] + (4 - 3\eta)K \} (1 + \frac{2\sigma R_o}{P_o})} \quad (\text{eqn. 7})$$

where

$\omega$  = angular frequency of excitation

$C_i$  = concentration of dissolved gas in the fluid far from the bubble

$C_o$  = equilibrium concentration of gas in the fluid

$K$  = thermal conductivity of the gas in the bubble

$P_{th}$  = threshold acoustic pressure amplitude at excitation frequency

Table 1 displays some results using equation 7.

Crum [Ref. 1] also discusses the equations that describe the change in size of an air bubble that is present in a liquid and experiencing a sinusoidal fluctuation in pressure. The expression for the rate of change of the bubble radius with time is given by [Ref. 1: eq. 13, p. 205]

$$\frac{dR_o}{dt} = \frac{Dd}{R_o} \left[ \left\langle \frac{R}{R_o} \right\rangle \left( 1 + \frac{4\sigma}{R_o} \right)^{-1} \left( \frac{C_i}{C_o} - \frac{\left\langle \left( \frac{R}{R_o} \right)^4 \left( \frac{P_g}{P_o} \right) \right\rangle}{\left\langle \left( \frac{R}{R_o} \right)^4 \right\rangle} \right) \right] \quad (\text{eqn. 8})$$

where  $d = RTCo/P_o$  with  $T$  as the absolute temperature in degrees Kelvin, and

$$\left\langle \frac{R}{R_o} \right\rangle = 1 + K\alpha^2 \left( \frac{P_A}{P_o} \right)^2 \quad (\text{eqn. 9})$$



TABLE 1. THRESHOLD ACOUSTIC PRESSURE AMPLITUDES FOR  
RECTIFIED DIFFUSION OF VARIOUS AIR BUBBLES IN AIR  
SATURATED WATER DRIVEN AT RESONANCE

BUBBLE RADIUS ( m)	RESONANCE FREQUENCY (kHz)	THRESHOLD PRESSURE (Pa)
100	31.4	1440
50	62.1	5690
10	303.8	8680
5	618.0	1.515 MPa *

\* carrier frequency = 2.65 mHz

$$\langle (\frac{R}{R_o})^4 \rangle = 1 + (3 + 4K)\alpha^2 (\frac{P_A}{P_o})^2 \quad (\text{eqn. 10})$$

$$\langle (\frac{R}{R_o})^4 (\frac{P_g}{P_o}) \rangle = [1 + (4 - 3\eta)K\alpha^2 (\frac{P_A}{P_o})^2] (1 + \frac{2\sigma}{R_o P_o}) \quad (\text{eqn. 11})$$

$$\beta^2 = \frac{\rho \omega^2 R_o^2}{3\eta P_o} \quad (\text{eqn. 12})$$

$$\alpha = [3\eta(1 + \frac{4\sigma}{3R_o P_o} - \beta^2)]^{-1} \quad (\text{eqn. 13})$$

$$K = \frac{\frac{(3\eta + 1 - \beta^2)}{4} + \frac{4\sigma}{3P_o R_o}}{1 + \frac{4\sigma}{3P_o R_o}} \quad (\text{eqn. 14})$$

where

D = diffusion constant

P<sub>A</sub> = applied acoustic pressure amplitude

P<sub>g</sub> = instantaneous pressure amplitude of the gas within the bubble

Bubbles can either grow or dissolve depending upon a variety of conditions as shown in Figure 4. Notice that it takes hundreds of seconds to cause a major change in bubble

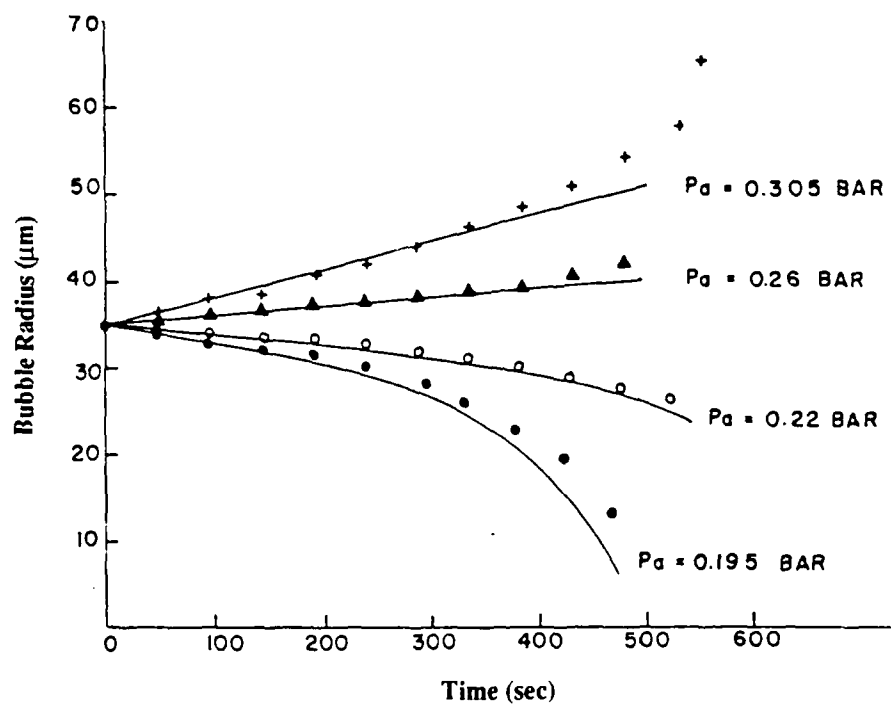


Figure 4. Rectified Diffusion Measurements by Crum, Solid Lines Representing Theory [Ref. 7:fig. 4, p. 207].

radius. Therefore, as long as the pressure amplitude used in the dual frequency method are at or below threshold amplitude and they are not applied for long periods of time, the dual frequency technique should not significantly affect the size of the bubbles being investigated.

#### **E. FREQUENCY RESPONSE, DAMPING, AND QUALITY FACTOR**

The frequency response and damping coefficient have been two of the most difficult characteristics of bubbles to accurately measure.

The total damping constant originates from three processes:

- thermal damping  $\delta_{th}$  due mainly to the thermal conduction between the gas in the bubble and the surrounding liquid
- Sound radiation damping  $\delta_{rad}$
- Viscous damping  $\delta_{vis}$  due mainly to viscous forces at the gas-liquid interface.

The total damping constant is the sum of the damping due to these three processes:

$$\delta = \delta_{th} + \delta_{rad} + \delta_{vis} \quad (\text{eqn. 15})$$

Prosperetti [Ref. 8] gives an elaborate discussion of the three terms. They are [Ref. 8: eq. 29+40, p. 72]

$$\delta_{vis} = \frac{4\mu}{\omega_p R_o^2} \quad (\text{eqn. 16})$$

$$\delta_{rad}^2 = \frac{\omega R_o}{c} = k R_o \quad (\text{eqn. 17})$$

$$\delta_{th} = 18\gamma(\gamma - 1) \frac{P_i(R_o)}{\rho w X_g} \frac{\theta A_+ - 2}{\theta^2 [0 + 3(\gamma - 1)A_-]^2 + 9(\gamma - 1)^2 (\theta A_+ - 2)^2} \quad (\text{eqn. 18})$$

with

$$X_g = \frac{K_g}{\rho_g C_{pg}} \quad (\text{eqn. 19})$$

$$A_{\pm} = \frac{\sinh \theta \pm \sin \theta}{\cosh \theta - \cos \theta} \quad (\text{eqn. 20})$$

where

$c$  = speed of sound of fluid

$P_i(R_o)$  = pressure acting on the inner side of the bubble surface

$\theta$  = ratio of the bubble radius to the gas thermal diffusion length

$X_g$  = thermal diffusivity of the gas

$K_g$  = thermal conductivity of the gas

$P_g$  = density of the gas

$C_{pg}$  = specific heat at constant pressure

For the low frequencies, equation 16 shows that viscous damping dominates at small radius. In contrast, equation 18 shows that thermal damping dominates at larger radius. Equation 17 shows that the acoustic contribution is negligible at low frequency. The reader is referred to [Ref. 8] for a more complete discussion.

For oscillations of a bubble, the quality of factor  $Q$  is [Ref. 5: eq. 23, p. 1657]

$$Q = \frac{f_0}{f_2 - f_1} \quad (\text{eqn. 21})$$

where  $f_1$  and  $f_2$  are the two frequencies below and above resonance at which the average sound power radiated by bubble has dropped to half its resonance value. The total damping constant is also defined as the reciprocal  $Q$  of the bubble,  $\delta = 1/Q$ . Measurements of the bubble response can therefore yield .

### III. APPARATUS AND MEASUREMENTS

The first step toward accomplishing the goal of this thesis is to design an apparatus which utilizes the dual frequency method to study bubbles in a fluid. The design and use of the device is described in this chapter.

#### A. DESIGN CONSIDERATIONS

It is proposed to use the dual frequency technique to determine the sizes and responses of bubbles in the range 10 to 125  $\mu\text{m}$  radius. Since it is important that the diameter of the bubble be small with respect to the wavelength associated with the frequency  $f_1$ , a maximum carrier frequency of approximately 3 MHz is necessary to insure that the acoustic wavelength is at least four times the size of the largest bubble radius of 125  $\mu\text{m}$ . Radii from 125  $\mu\text{m}$  down to 10  $\mu\text{m}$  correspond to resonance frequencies from approximately 30 kHz to 330 kHz. Assuming that harmonics of  $f_1$  higher than the fifth will be insignificant leads to a minimum carrier frequency of about six times the highest bubble resonance or approximately 2 MHz. Therefore, a value of 2.65 MHz was chosen for  $f_1$  in the experiment.

The frequency of  $f_2$  of the other sound field will be swept from below to above the resonance frequency of the bubble. The swept rate must be slow enough to insure that the bubble reaches its steady state response at a given frequency. However the sweep rate must be high enough and the amplitude low enough so that the bubble does not grow due to rectified diffusion.

To be able to make measurements on a single bubble over a prolonged period of time, it is necessary that the bubble remain in the same place during the interrogation process. To accomplish this requirement, the bubble will be levitated in the sample region. The levitation field can also serve as the driving field in order to study rectified diffusion and bubble damping. A discussion of bubble levitation is given in [Ref. 4].

From the definition of all the above mentioned features, the use of the dual frequency method requires that the device has the following capabilities:

- A method of generating bubbles
- A method of levitating bubbles
- A method of producing a carrier frequency  $f_1$  and an exciter frequency  $f_2$
- A method of receiving the pressure signals from the bubble and producing a frequency spectrum of the received signal



## **1. Generating Bubbles**

A method for generating bubbles of radii sizes 10 to 125  $\mu\text{m}$  is necessary for this thesis. A way to generate bubbles of such sizes is to stimulate rectified diffusion of microbubbles already present in the saturated fluid. Once the bubbles are at the desired size, the amplitude of the driving field is reduced, thereby halting the growth.

## **2. Bubble Levitation**

Since the position of the bubble is important in this device, it is desirable to hold the bubble at precisely the same position. This can be accomplished with the levitation cell described below.

From a vertical plexiglass tube as a container for the fluid, transducers can be employed to excite a standing wave pattern along the length of the tube. A bubble can be levitated in the standing wave pattern by adjusting the pressure amplitude to counteract the buoyancy force of the bubble. By selecting the appropriate transverse normal model, with maximum velocity (minimum pressure) at the walls and minimum velocity (maximum pressure) at the center, the bubble can be held at the center of the cylinder. A frequency that produces a normal model (0, 1, 4) for a cylinder (0, r, z) as presented in [Ref. 9] will produce such a result.

### **3. Carrier and Exciter**

The two sound fields required in the dual frequency method can be generated by commercially available immersion transducers. The carrier transducer must be capable of generating sufficient amplitudes at the specified carrier frequency  $f_1$ . On the other hand, the exciter transducer must be capable of generating signals over a range of frequencies,  $f_2$ , at constant amplitude.

### **4. Reception and Display of Received Signal**

Once the bubble has been excited, a transducer is needed to record the resulting pressure radiated by the bubble as a function of the frequency  $f_2$ . As described in the theory section, a bubble will radiate much higher amplitudes at its resonance frequency  $f_0$  than at any other frequencies. This received signal can be displayed with the help of a frequency spectrum analyzer.

## **B. EXPERIMENTAL SET-UP**

Following the establishment of the design considerations, it is now possible to build the device. This section will describe the transducers employed, the actual device, the electronic equipment, and the schematic of the total system.

## 1. Transducers

As described in paragraph A, four transducers are required. A 3-inch diameter, 1-inch long, piezoelectric ceramic type is used to establish standing waves within the plexiglass cylinder of same diameter. Located at the top of the cylinder as shown in Figure 5, it is used at a frequency of 21.90 kHz to excite the desired normal model in the cylinder.

Stuck to the bottom of the plexiglass cylinder, a Panametrics V301 1-inch diameter circular piezoelectric immersion transducer (serial number 93596) is used as the exciter. The selection of this transducer was based upon the fact that the frequency response over the range of 20 to 100 kHz is flat, within 5dB. This transducer could have been located almost anywhere as long as the bubble can be excited. To demonstrate this, a small piezoceramic hydrophone will be used as the exciter later to compare results from two different exciters.

Two Panametrics V323, 0.25-inch diameter circular piezoelectric immersion transducers are used as the carrier (serial number 923564) and the receiver (serial number 93566). These two transducers are located 6.0 cm from the top of the cylinder. They were placed in position by a plexiglass block

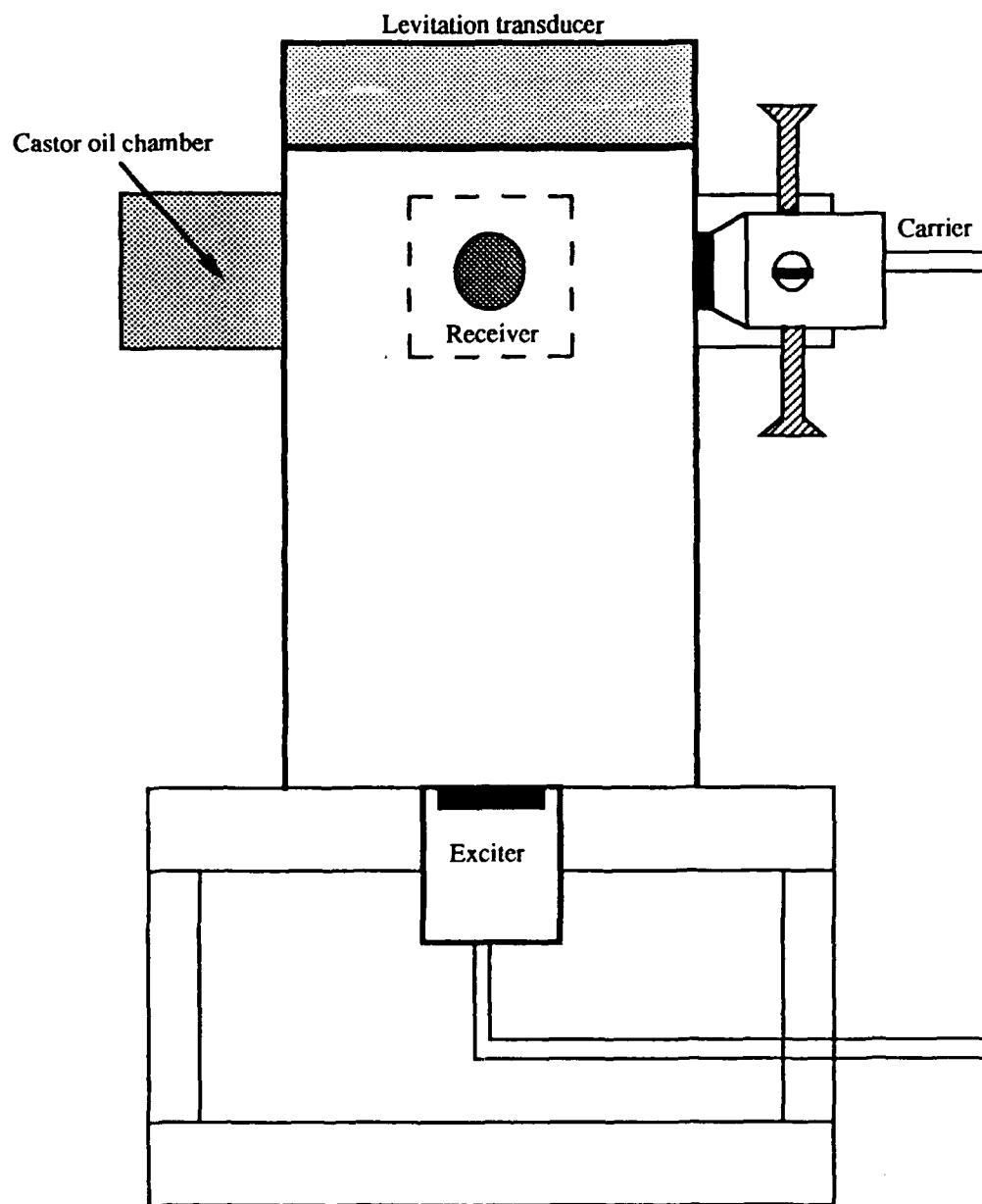


**Figure 5. Transducer Locations for Multi-Frequency Method**

formed to hold them with the help of four screws. Because the beamwidth of these two transducers is only 10 degrees in the frequency range used, precise alignment is necessary to ensure that both beam patterns intersect at the location of the bubble.

## **2. Apparatus**

After consideration of the requirements placed on transducer position discussed in the last paragraph, the transducers were attached to the cylinder at the positions shown in Figure 5. This arrangement enabled the experimenter to actually see the bubble, simplifying the task of centering the bubble between the carrier and receiver transducers.

The carrier transducer transmits a CW sinusoidal signal at 2.65 MHz. To reduce the amount of reflection of this signal, a castor oil chamber was placed directly across from the carrier transducer. The castor oil was kept separate from the water in the test cell by means of a thin mylar window.

The brass plate used to incase the exciter transducer also served as the bottom of the cylinder insuring a pressure antinode at the bottom of the chamber. The overall dimensions of the actual chamber are 17.8 cm high by 7.6 cm diameter.

### 3. Electronic Equipment

This paragraph will detail the electronic equipment shown in Figure 6.

To produce and levitate the bubble, a HP8904A Multifunction Synthesizer is used to produce a 21.90 kHz sine wave. This signal is amplified with an Amplifier Research model 100A15 power amplifier which has a variable gain control. The output was monitored on a Tektronix 2445A oscilloscope.

The exciter signal is generated by a HP3314A Function Generator in the sweeping model from 20 kHz to 100 kHz. This signal is amplified by an Amplifier Research model 50A15 amplifier. A low pass RC filter was used to eliminate frequency components above 500 kHz, therefore reducing the changes of interference with the carrier. The Tektronix 2445A oscilloscope was also used to monitor the signal.

The carrier signal is a 2.65 MHz sinusoidal waveform. The signal is generated by a HP8640B Signal Generator which has a very good spectral purity. This purity is required because the sideband signals produced by the dual frequency method flank the carrier on a spectral plot.

The received signal is amplified with a Minicircuits model ZHL-32A preamplifier having a gain of 27dB +/- 2dB over



the range of interest. The amplified signal is then sent to a HP3585A Spectrum Analyzer. To reduce the range of the required frequency sweep, thereby increasing the resolution, only the sum frequency would be swept and displayed. For example, with a carrier of 2.65 MHz and an exciter sweeping from 20 to 100 kHz, the spectrum analyzer will sweep from 2.67 to 2.75 MHz. The resulting spectrum would then be plotted on the HP7090A plotter. The sweep time of the analyzer was set to match that of the exciter.

#### **4. Sample Fluid**

The fluid used in these measurements is deionized, air saturated water. A thermometer is used to record the room temperature and a tensiometer to measure the surface tension of the water. Between each data run, the water was vigorously shaken insuring an air saturated sample.

#### **5. Calibration**

Due to the complexity of the acoustic field in the cylinder caused by the three active transducers, it was judged inappropriate to determine the absolute, free field, calibrations for each transducer. Introducing a small calibrated hydrophone and measuring the actual field present at the location of the bubble was a more feasible and accurate way of determining the acoustic pressures at the bubbles.



Two hydrophones were used: an LC-10 (serial number B-907) and a small transducer built from a Channel 5500 thin walled cylindrical ceramic reversible transducer. A full reciprocity calibration as presented in Chapter II of [Ref. 2] was executed on both hydrophones producing a relatively ( $\pm 1$ dB) accurate receiver sensitivity from 5 kHz to 100 kHz. It was then possible to insure that the carrier and exciter would not produce pressure sufficient to cause rectified diffusion. When rectified diffusion was desired, it was produced with the 21.90 kHz levitation field. A scale marked on the variable gain control on the amplifiers indicated the actual pressure amplitudes acting on the bubble.

## **6. Procedures**

The bubble radius was measured using both the rise time method and the rectified diffusion method. The former one requires that the carrier and exciter pressure amplitudes be zero while allowing the bubble to rise on its own after turning off the levitation transducer. The time for the bubble to travel between two marks separated vertically by 25 mm placed on the plexiglass is measured using a stopwatch.

For the latter case, rectified diffusion method, the bubble is levitated to the desired position. Next the desired pressure amplitude is applied to the bubble by the levitation

sound field. At approximately every 100 seconds, the bubble radius is measured using the dual frequency method with the use of the carrier and exciter transducers. This process takes, on the average, 15 seconds.

#### **IV. RESULTS AND DISCUSSION**

The results of measurements of bubble resonance frequency (bubble radius), rectified diffusion rates, and bubble response using the device described in the previous chapter are presented in this chapter. Before presenting these results, a brief discussion of the output display of the spectrum analyzer is presented. Finally, a discussion of the possibilities of measuring the damping coefficients of bubble using the dual frequency method will be presented.

##### **A. SPECTRUM ANALYZER**

The primary detection device for this experimental setup is the HP3585A Spectrum Analyzer. This spectrum analyzer sweeps through a specified frequency range and displays the response as a graph of amplitude versus frequency.

With all transducers off, the spectrum would be a horizontal line with ambient noise fluctuations of  $\pm 2$  dBV. If a bubble is present at the desired position and both the levitation frequency of 21.90 kHz and the carrier frequency of 2.65 MHz are being transmitted, the display under of the received signal under these conditions is similar to that shown in Figure 7. The spectral lines are those corresponding

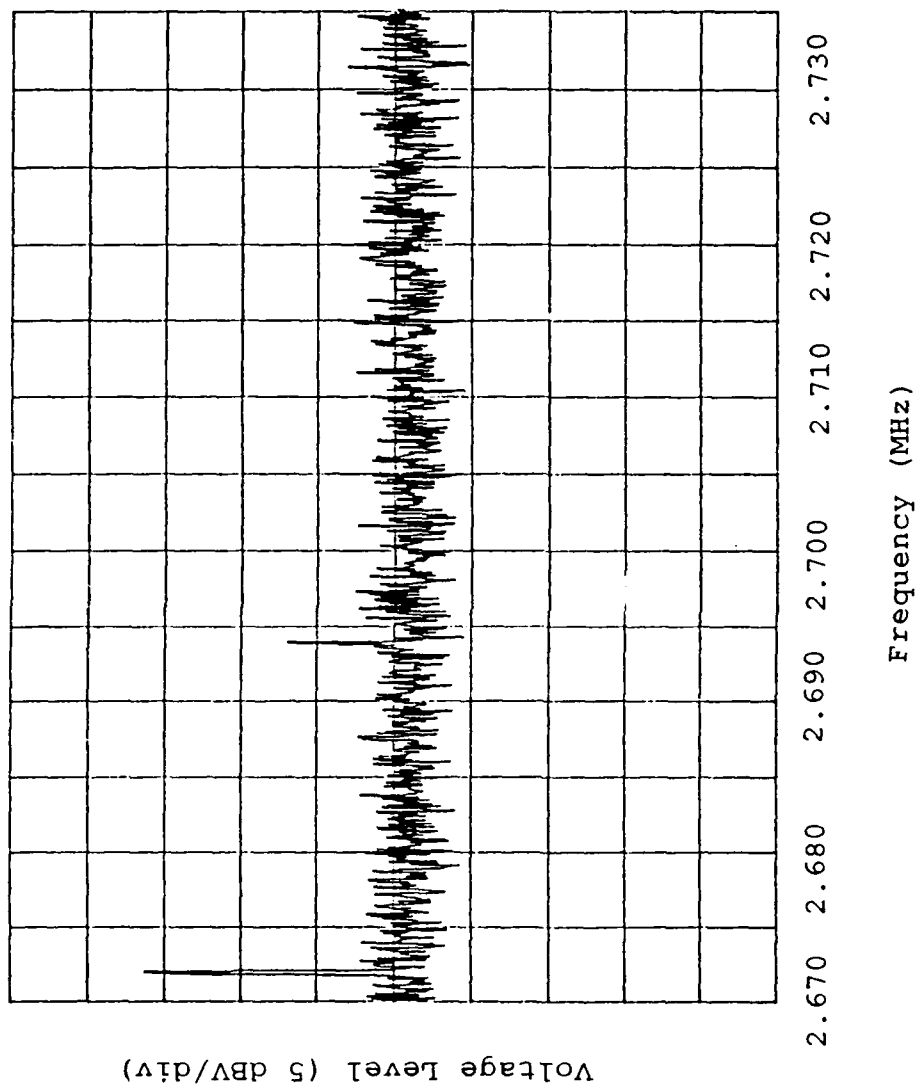


**Figure 7. Frequency Spectrum with Bubble Carrier and Levitation Transducers on.**

to the frequency summation of the carrier  $f_1$  and the levitation  $f_3$  signals  $(f_1+f_3)$  and its second harmonic  $(f_1+2*f_3)$ . Figure 8 is the same display after the exciter transducer has been activated. The spectral line displaying the summation of the carrier frequency and the bubble resonance frequency  $(f_1+f_0)$  is easily observed. From observations, the bubble resonance frequency is obtained. It should be noted that a range of frequencies on either side of  $(f_1+f_0)$  are also present in the display.

#### **B. BUBBLE RADIUS**

The frequency of highest amplitude, other than the levitation frequency, allows determination of the bubble's resonance frequency. From the resonance frequency, equation 4, and Figure 2, the bubble radius can be obtained. The bubble rise time, described by equation 5, can be used to independently determine the bubble radius. Figure 9 shows the results of a large number of such comparisons between the two methods. After many attempts in measuring the rise time of the bubble through 25 mm of water, it was determined that time was accurate to within  $\pm 5\%$ . This error is displayed on the horizontal axis of Figure 9. Perfect agreement would correspond to all the data points falling on a line having a slope of one. The slope, determined by a least square fit to

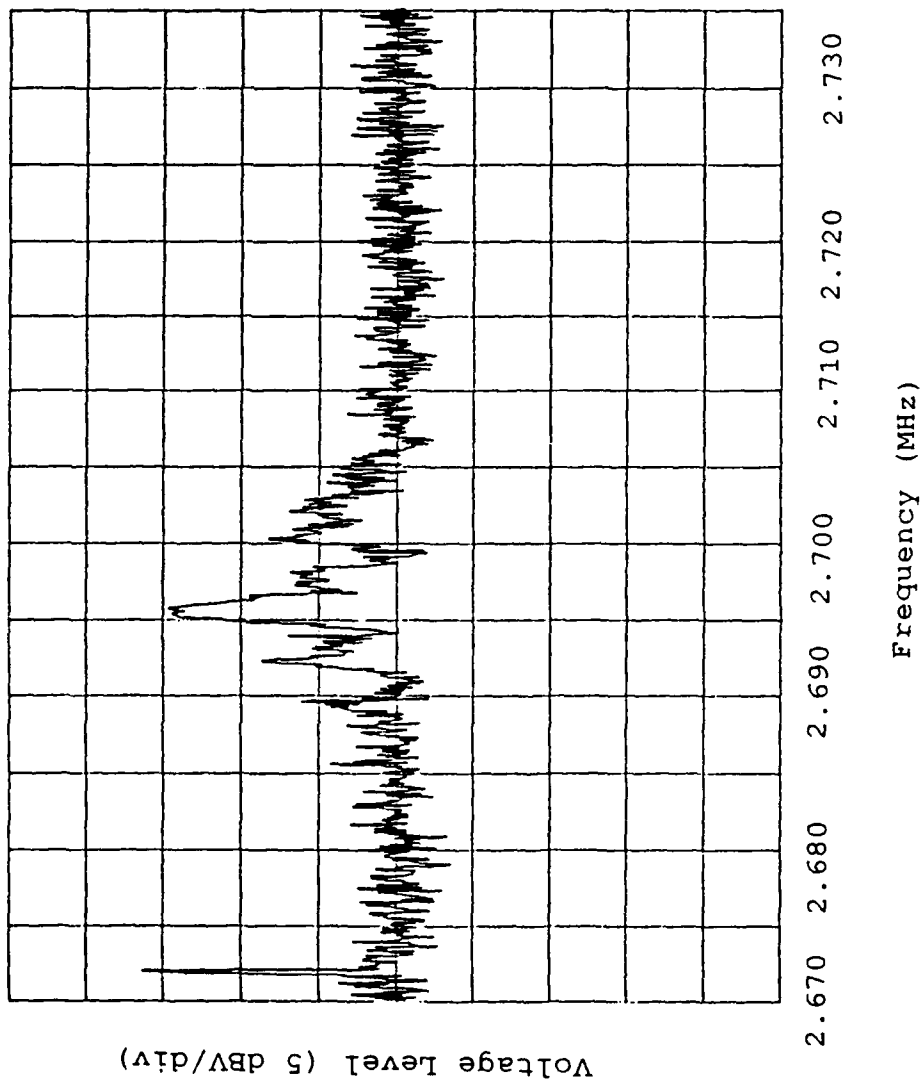


**Figure 8. Frequency Spectrum with Bubble Carrier, Exciter and Levitation Transducers On.**

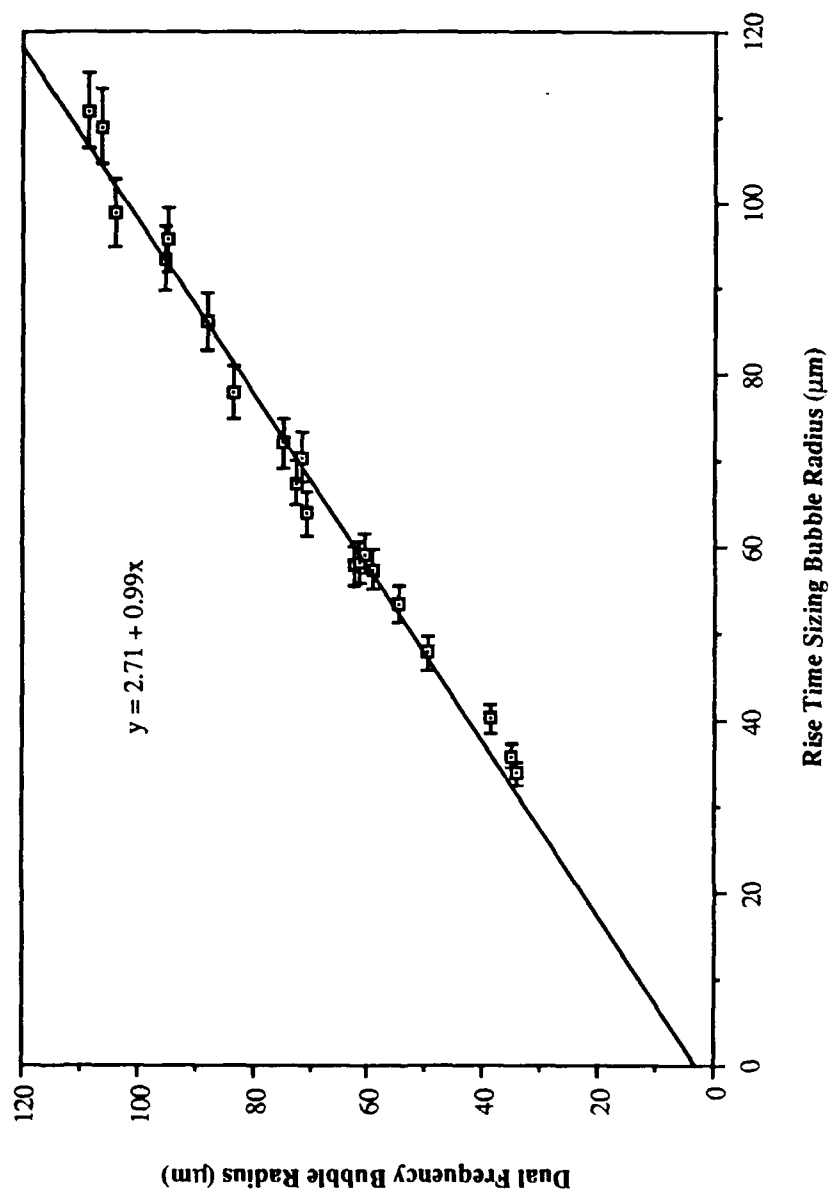


Figure 9. Bubble Radius as Determined from Two Different Methods

the data, is 0.99. Therefore, the two methods agree to within approximately 1% in most cases.

### C. RECTIFIED DIFFUSION

In a second verification, the dual frequency method was used to measure the growth of bubbles due to rectified diffusion. These measurements are done for bubbles with radius in the proximity of 50  $\mu\text{m}$  which can be observed with the naked eye. For such a bubble of 50  $\mu\text{m}$  radius, equation 7 gives a rectified diffusion threshold of approximately 23.0 kPa. Three different rectified diffusion rates were studied in this thesis. The first is for the case of a negative rectified diffusion rate, in which the bubble dissolves. A pressure amplitude of 7.6 kPa was applied to the bubble using the levitation transducer. Figure 10 shows the measured values for a bubble reduction in size from 61.9 to 44.0  $\mu\text{m}$  in a span of 585 seconds. The different type of data points refer to different bubbles. The solid line is the direct result of the integration of equation 4.

The next rectified diffusion measurement is for the case when the sound field is near the threshold value. In this case, little change in radius is expected. Figure 11 overlays



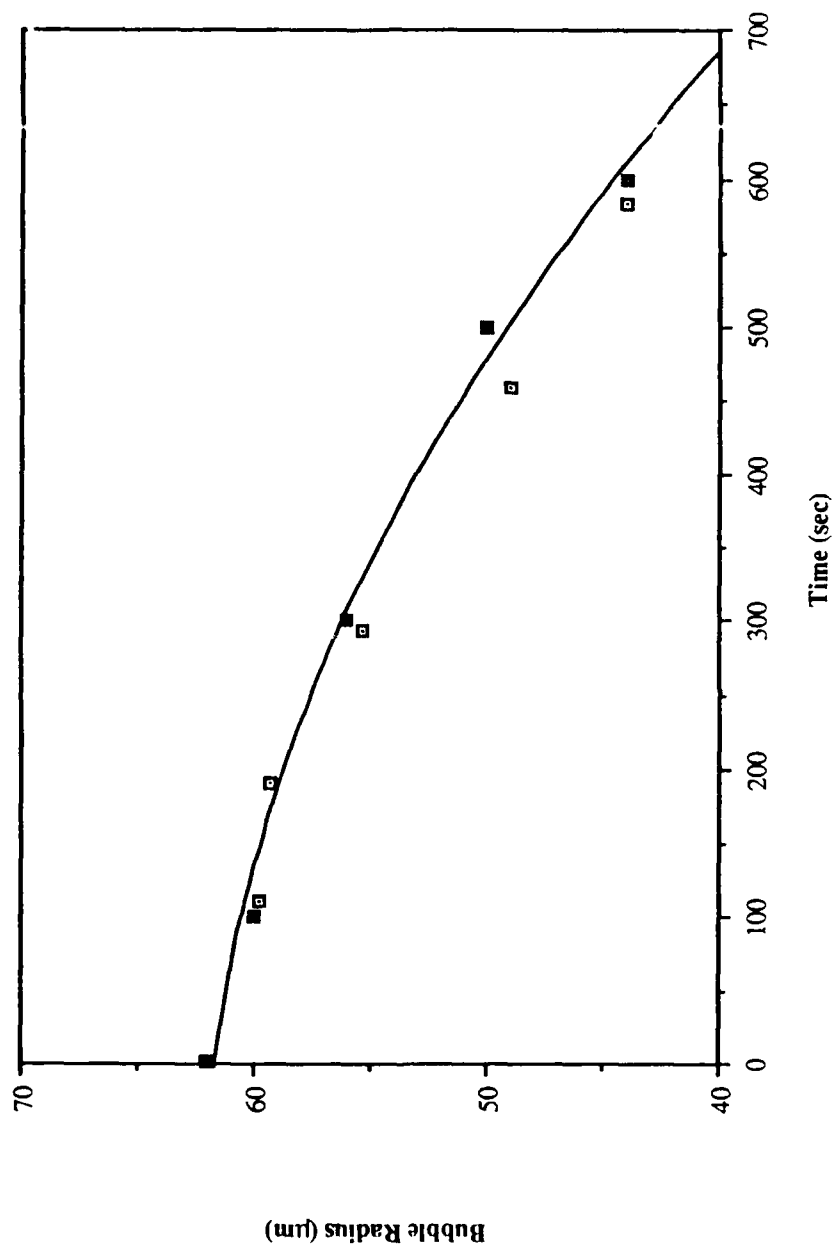


Figure 10. Behavior of Air Bubble in Water when Applied Sound Field Less than Rectified Diffusion Threshold,  $f = 21.9$  kHz,  $P = 7.6$  kPa.

the first five spectrum analyzer displays of such a case, while Figure 12 shows the radius versus time.

The final rectified diffusion measurement is for the case when the sound field is well above the threshold value. Figures 13 and 14 display the results when the pressure amplitude is 30.4 kPa. Data are shown for four different bubbles in Figure 14. The solid line in Figure 14 is, again, the integration of equation 8.

These results clearly demonstrate the ability to measure rectified diffusion using the dual frequency method. The reader should compare Figures 10, 12, and 14 with similar measurements made visually by Crum, Figure 4.

#### **D. DAMPING COEFFICIENTS**

While it is shown that the device is very effective in measuring the properties of the bubble such as its radius and rectified diffusion threshold and rates, some very important additional information can be retrieved from the spectral response. In particular, it should be possible to retrieve the frequency response and thereby determine the damping coefficient, through the quality factor. Determining a quality factor requires a relatively smooth response which is not yet provided by this device. The explanation for this uneven response rests in the fact that the pressure produced

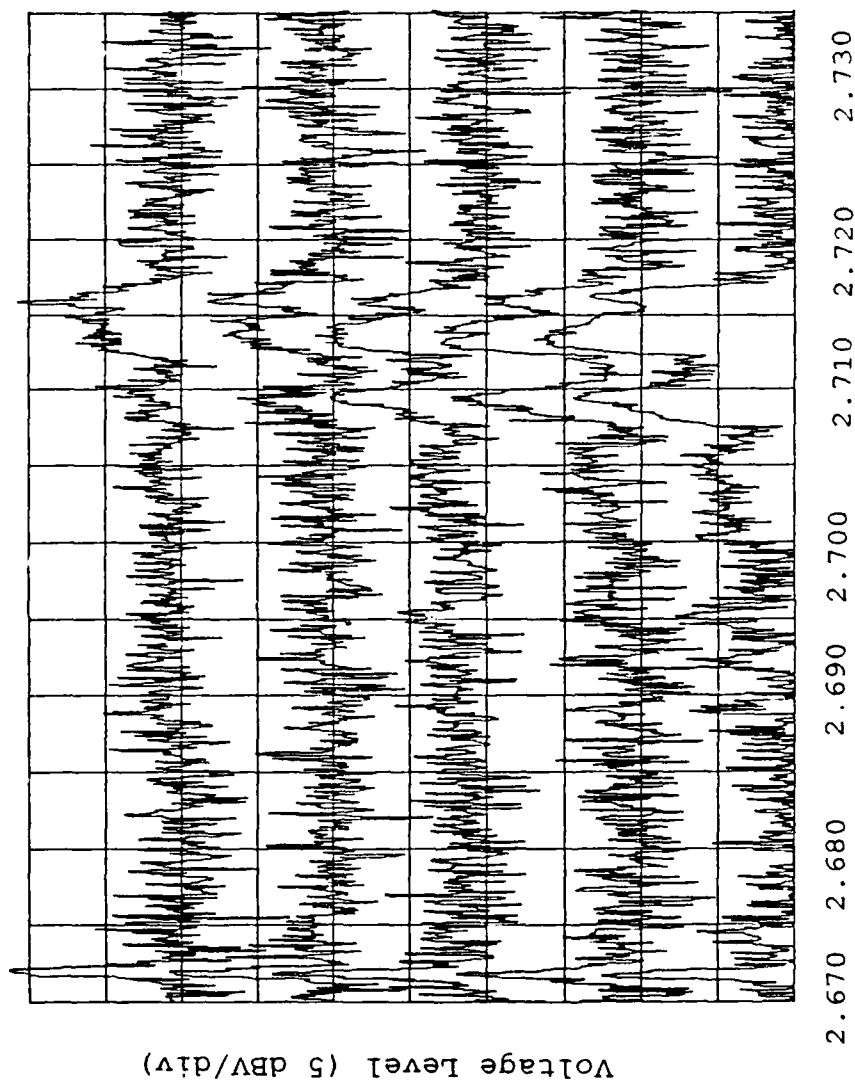


Figure 11. Superposition of Five Frequency Spectrums, 100 Seconds Apart, at Rectified Diffusion Threshold.

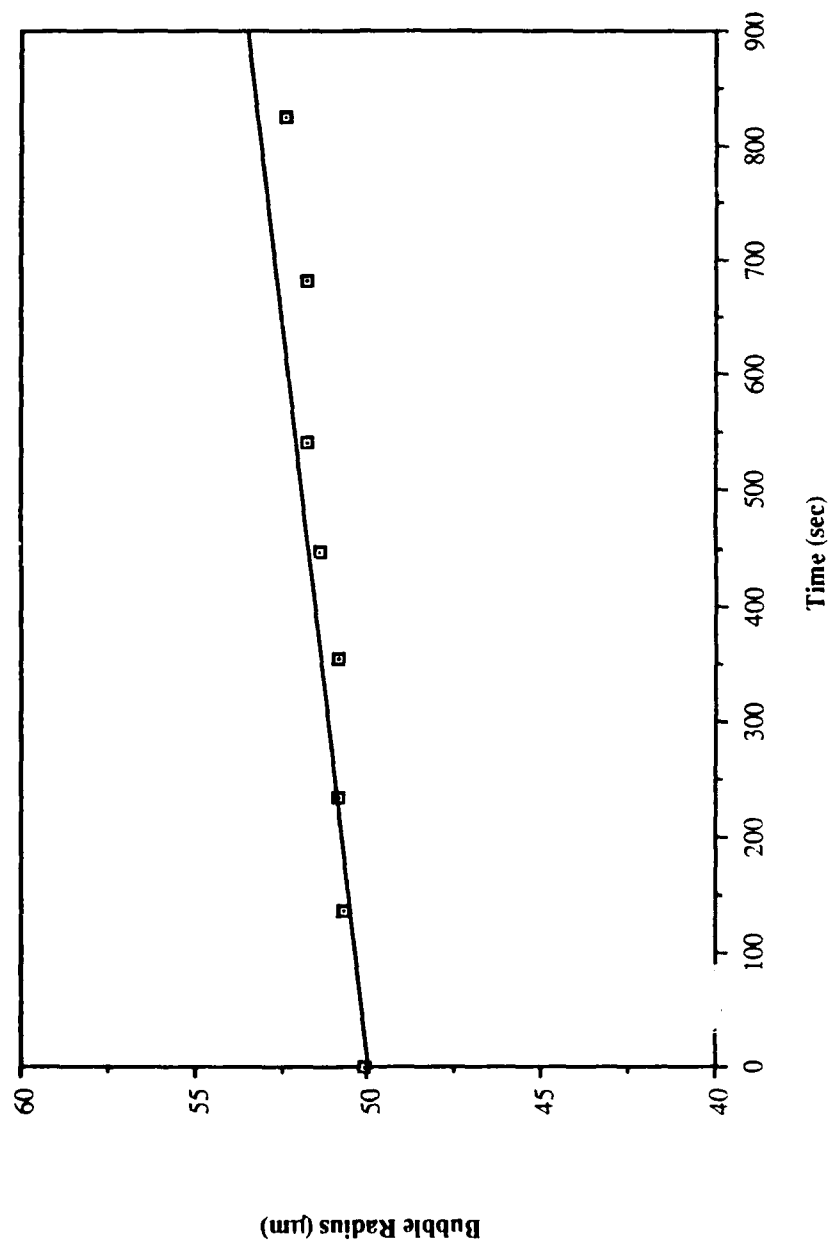


Figure 12. Bubble Radius Variations at Rectified  
Diffusion Threshold for Air Bubble in Water,  
 $f = 21.9$  kHz,  $P = 23.0$  kPa.

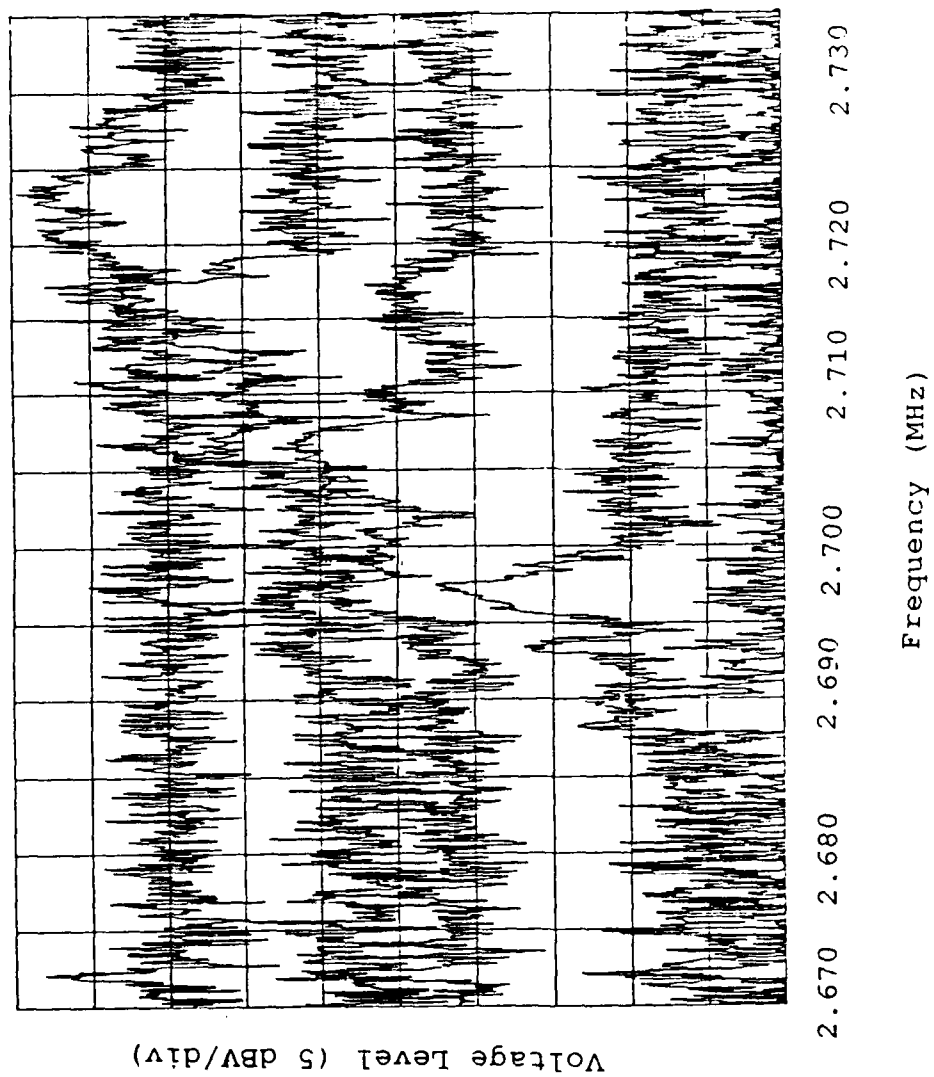


Figure 13. Superposition of Five Frequency Spectrums, 100 Seconds Apart, for Positive Rectified Diffusion.

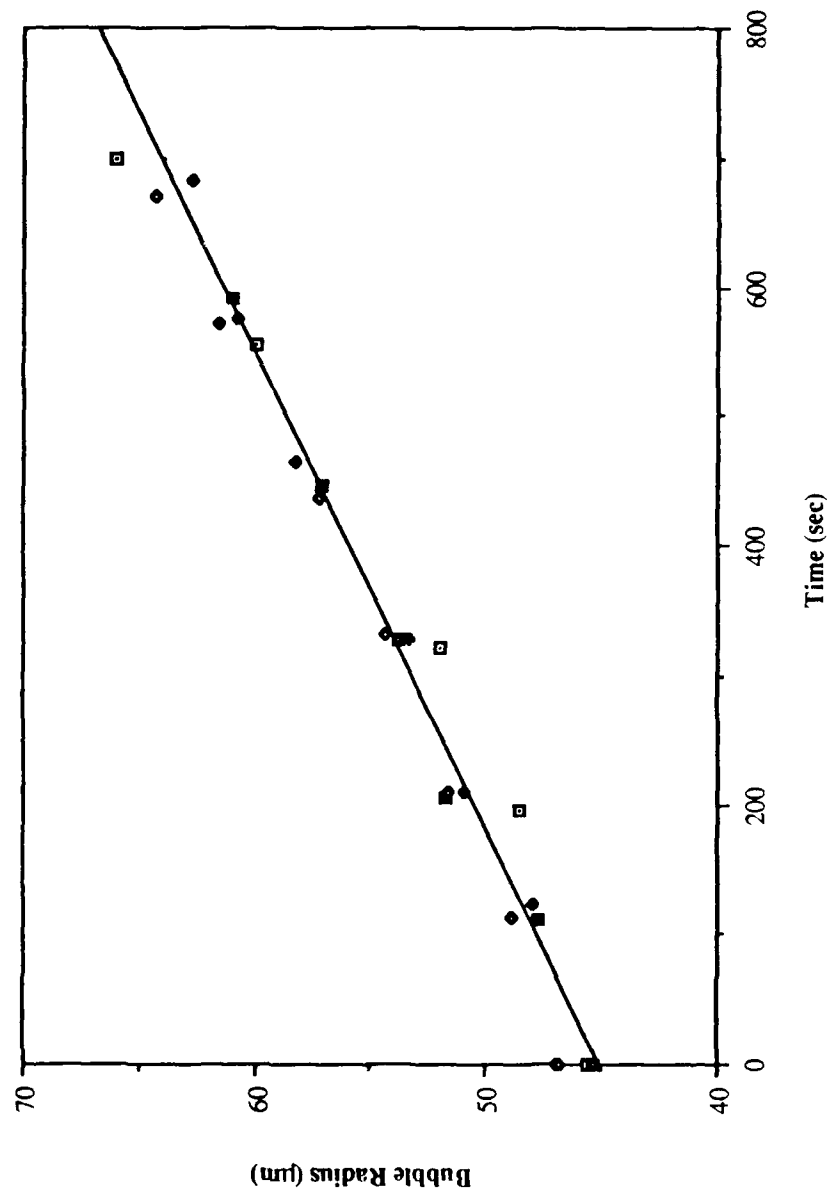


Figure 14. Behavior of Air Bubble in Water when Applied Sound Field Greater than Rectified Diffusion Threshold,  $f = 21.9$  kHz,  $p = 30.4$  kPa.

by the exciter transducer is not flat once it is incorporated in the device. This is probably the result of reflection from the walls of the cylinder and the surface of the water. Fortunately, this problem can be avoided by using the small piezoelectric ceramic hydrophone (originally used for calibration purposes) as the exciter transducer. Figure 15 displays the difference between the received signal amplitude with the small ceramic transducer as a exciter transmitter placed directly in the chamber about 25 mm from the position of the levitated bubble (heavy line) and the Panametrics V301 exciter (thin line). Figures 16 and 17 display the improvement accomplished by such a change in exciter.

Another way to use the dual frequency method to measure the damping coefficient is to use equation 2 which describes the relation between the acoustic pressure amplitude at the frequency ( $f_1+f_2$ ) and the damping coefficient. Unfortunately, this method is nonreliazable in this thes's due to the inability of achieving an absolute pressure amplitude reading at such high frequency with the equipment available.

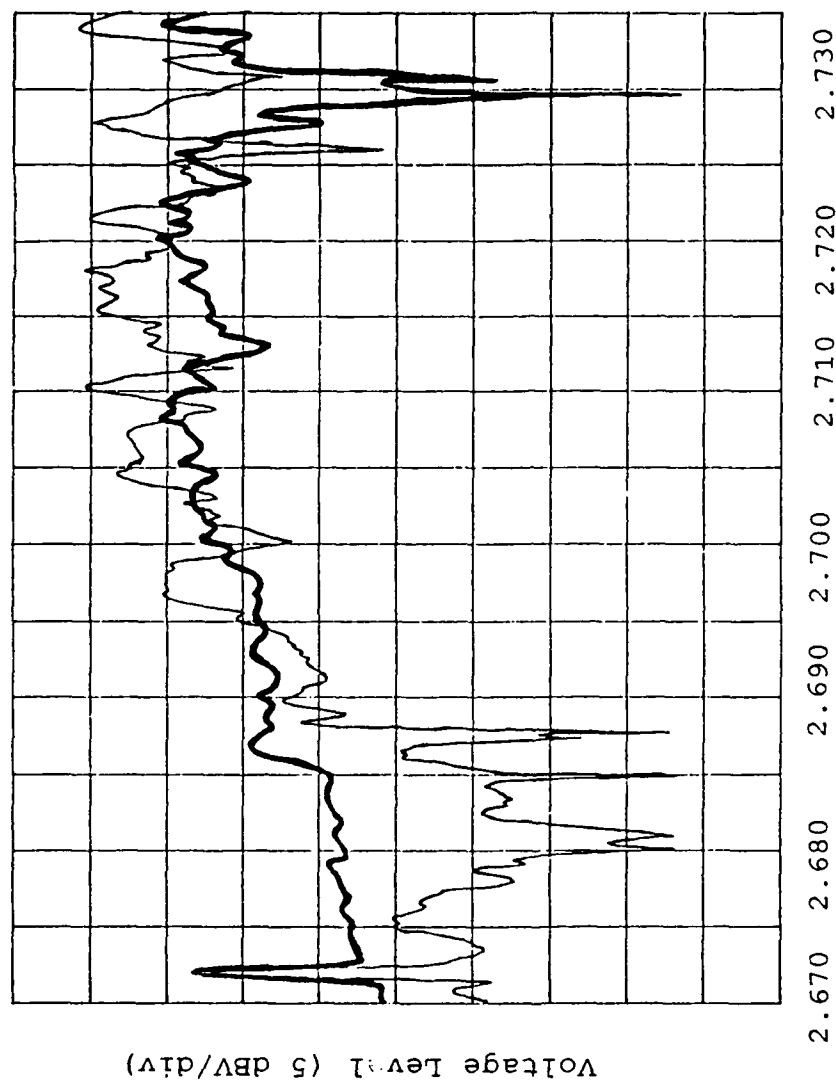
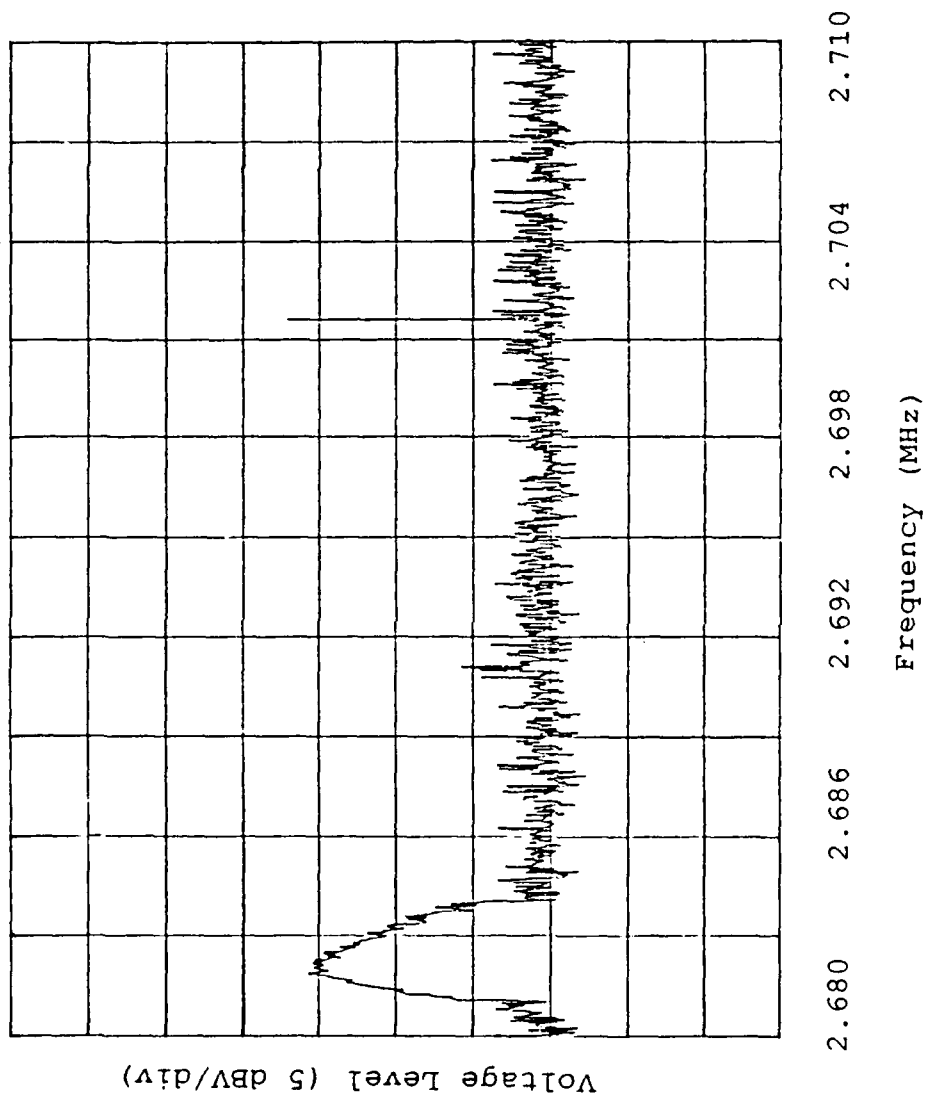
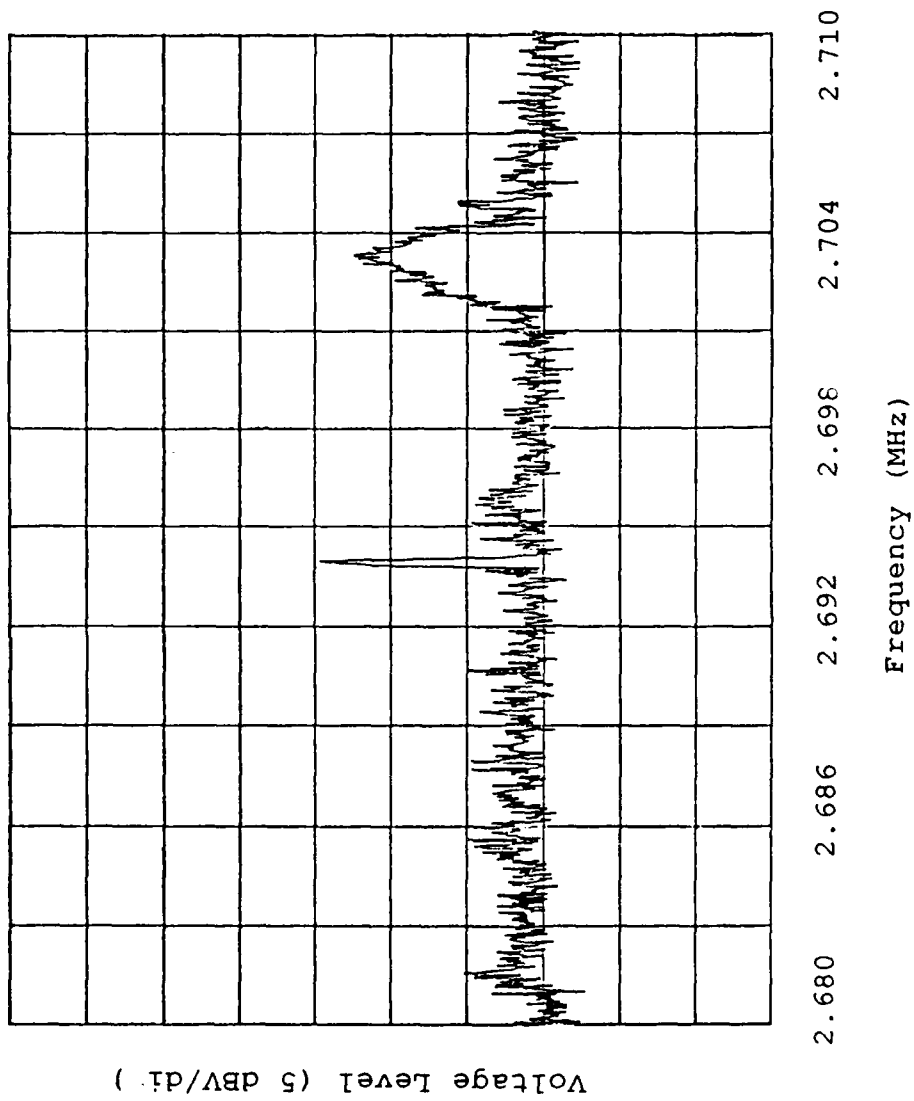


Figure 15. Comparison of Exciters, Small Ceramic Transducers (heavy line), Panametrics V301 (thin line).





**Figure 16. Bubble Response from Small Ceramic Exciter.**



**Figure 17. Bubble Response from Small Ceramic Exciter**

## V. SUMMARY

The goals of developing and testing a new device for measuring bubble properties, based on the dual frequency method, have been accomplished. The experimental setup has demonstrated the ability to detect single bubbles with resonance frequencies from 30 to 100 kHz. From these resonance frequencies, the bubble radius was computed and the accuracy of this determination was verified by comparison to radii determined from the rise time method. This comparison gave an average difference of approximately 1%.

The ease and accuracy in measuring rectified diffusion rates, negative or positive, using the dual frequency method was also demonstrated.

The use of the method also has great potential for measuring the frequency response and damping coefficient of bubbles. The response in the sidebands has received very little attention previously. It remains to be seen what information can be obtained from responses such as shown in Figures 16 and 17.

There are also a number of areas for application of this technique such as to study the effect of varying a fluid's viscosity or surface tension on a bubbles damping constant.

#### LIST OF REFERENCES

1. Crum, L. A., "Measurements of the Growth of Air Bubbles by Rectified Diffusion", *Journal of the Society of America (JASA)*, Vol 68(1), pp. 203-211, July 1980.
2. Bobber, R. J., *Underwater Electroacoustic Measurements*, Naval Research Laboratory, pp. 17-36, Washington, DC, 1970.
3. Newhouse, V. L. and Shankar, P. M., "Bubble Measurements Using the Nonlinear Mixing of Two Frequencies", *Journal of the Acoustical Society of America (JASA)*, Vol 75(5), pp. 1473-1477, May 1984.
4. Crum, L. A. and Prosperetti, A., "Nonlinear Oscillations of Gas Bubbles in Liquids: An Interpretation of Some Experimental Results" *Journal of the Acoustical Society of America (JASA)*, Vol 73(1), pp. 121-127, January 1983.
5. Devin, C., Jr., "Survey of Thermal, Radiation, and Viscous Damping of Pulsating Air Bubbles in Water", *Journal of the Society of America (JASA)*, Vol 31(12), pp. 1654-1667, December 1959.
6. Technical Report for Office of Naval Research, Contract N00014-84-c-0193, *Mie Scattering as a Technique for the Sizing of Air Bubbles*, by G. M. Hansen and L.A. Crum, pp. 5-7, 1 June 1983.
7. Crum, L. A., "Acoustic Cavitation Series: Part Five, Rectified Diffusion", *Ultrasonics*, pp. 215-223, September 1984.
8. Prosperetti, A., "Bubble Phenomena in Sound Fields: Part One:", *Ultrasonics*, pp. 69-76, March 1984.
9. Kinsler, L. E., Frey, A. R., Coppens, A. B., and Sanders, J. V., *Fundamentals of Acoustics*, pp. 389-391, 3rd Edition, Wiley, 1982.

# INITIAL DISTRIBUTION LIST

1. Defense Technical Information Center 2  
Cameron Station  
Alexandria, Virginia 22304-6145
2. Library, Code 0142 2  
Naval Postgraduate School  
Monterey, California 93943-5002
3. Professor Anthony A. Atchley, Code 61Ay 5  
Physics Department  
Naval Postgraduate School  
Monterey, California 93943-5002
4. Professor S. L. Garrett, Code 61Gx 1  
Physics Department  
Naval Postgraduate School  
Monterey, California 93943-5002
5. Chairman 1  
Department of Physics, Code 61  
Naval Postgraduate School  
Monterey, California 93943-5002
6. Dr. Larry Crum 1  
National Center for Physical Acoustics  
University, Mississippi 38677
7. National Defense Headquarters 1  
101 Colonel By Drive  
Ottawa, Ontario  
Canada, K1A 0K2  
ATTN: DMCS-3
8. Defense Research Establishment Atlantic 3  
F.M.O. Halifax  
Halifax, Nova Scotia  
Canada, B3K 2X0  
ATTN: Capt J.A.R. Perron

9. Acoustic Data Analysis Center  
F.M.O. Halifax  
Halifax, Nova Scotia  
Canada, B3K 2X0  
ATTN: Commanding Officer

1